Molecular Cell
Article

Regulation of Set9-Mediated H4K20 Methylation by a PWWP Domain Protein

Yu Wang,[1] Bharat Reddy,[1] James Thompson,[2] Hengbin Wang,[3] Ken-ichi Noma,[4] John R. Yates III,[2] and Songtao Jia[1,*]
[1]Department of Biological Sciences, Columbia University, New York, NY 10027, USA
[2]Department of Cell Biology, The Scripps Research Institute, La Jolla, CA 92037, USA
[3]Department of Biochemistry and Molecular Genetics, The University of Alabama at Birmingham, Birmingham, AL 35294, USA
[4]Laboratory of Biochemistry and Molecular Biology, National Cancer Institute, Bethesda, MD 20892, USA
*Correspondence: jia@biology.columbia.edu
DOI 10.1016/j.molcel.2009.02.002

SUMMARY

Methylation of histone H4 lysine 20 (H4K20me) is essential for recruiting checkpoint proteins 53BP1/Crb2 to DNA lesions and subsequent activation of a DNA-damage checkpoint. In fission yeast, Set9 (spKMT5) catalyzes mono-, di-, and trimethylation of H4K20. However, the mechanisms that regulate Set9 function are poorly understood. Here, we identified a PWWP domain protein Pdp1 as a Set9-associated factor. Pdp1 binds to histones and is required for Set9 chromatin localization. Yeast cells without Pdp1 were deficient in all three states of H4K20me, sensitive to genotoxic treatments, and impaired in Crb2 recruitment. The PWWP domain of Pdp1 binds to H4K20me, and mutations within the PWWP domain that abrogated this interaction in vitro reduced both the association of Set9 with chromatin and the extent of H4K20me in vivo. These results demonstrate that the PWWP domain is a new methyl-lysine recognition motif that plays important roles in epigenetic regulation.

INTRODUCTION

In eukaryotic cells, genomic DNA is folded with histone and nonhistone proteins into chromatin. The building block of chromatin is the nucleosome, which contains 146 base pairs of DNA wrapped around an octamer of histones (two each of H2A, H2B, H3, and H4) (Luger et al., 1997). Covalent modification of histones and DNA along with chromatin remodeling are essential features of an intricate epigenetic system for the regulation of chromatin structure and function. These epigenetic modifications not only affect compaction of DNA in the nucleus but also play important regulatory roles in almost every aspect of DNA metabolism including transcription, replication, recombination, and DNA repair (Berger, 2007; Downs et al., 2007; Groth et al., 2007; Kouzarides, 2007; Li et al., 2007).

Lysine methylation is one of the most intriguing histone modifications due to its remarkable specificity (Martin and Zhang, 2005). It is detected on many histone lysines, each of which can be mono-, di-, or trimethylated (me1, me2, and me3, respectively). These highly conserved modifications normally cluster within specific regions of the genome to organize chromosomes into distinct structural and functional domains. For instance, H3K4me (methylation of histone H3 lysine 4) is usually associated with actively transcribed genes, whereas H3K9me is enriched at transcriptionally repressed heterochromatin structures (Litt et al., 2001; Noma et al., 2001). In addition to controlling gene expression, H3K79me and H4K20me are required for efficient recruitment of checkpoint proteins 53BP1/Crb2 to sites of DNA damage (Botuyan et al., 2006; Du et al., 2006; Huyen et al., 2004; Sanders et al., 2004). The subsequent activation of DNA-damage checkpoints transiently arrests the cell cycle to allow DNA repair, thus preventing the propagation of DNA lesions (Rouse and Jackson, 2002; Zhou and Elledge, 2000).

The distinct distribution profiles of various histone lysine methylations across genomes suggest that the enzymes that catalyze histone lysine methylation, the histone methyltransferases (HMTases), are tightly regulated. Indeed, many HMTases form highly conserved complexes with other chromatin proteins to regulate their localization or activities. For example, the E3 ubiquitin ligase complex Cul4-Rik1 associates with the H3K9 HMTase Clr4 and regulates its localization to repetitive DNA elements to establish heterochromatin (Hong et al., 2005; Horn et al., 2005; Jia et al., 2005). The H3K27 HMTase E(Z)/EZH2 forms the polycomb repressive complex 2 (PRC2) that includes ESC/EED and SU(Z)12, which are essential for its HMTase activity (Cao et al., 2002; Czermin et al., 2002; Kuzmichev et al., 2002; Muller et al., 2002). In some cases, the associated proteins also regulate the processivity of HMTases. For instance, the association of mAM with ESET/SETDB1 is required for trimethylation of H3K9, and WDR5 of the MLL complexes is essential for trimethylation of H3K4 (Wang et al., 2003; Wysocka et al., 2005).

The methylation of H4K20 is involved in a diverse array of cellular processes, such as organizing higher-order chromatin, maintaining genome stability, and regulating cell-cycle progression (Fang et al., 2002; Julien and Herr, 2004; Karachentsev et al., 2005; Nishioka et al., 2002; Rice et al., 2002; Sakaguchi and Steward, 2007; Schotta et al., 2004, 2008). Multiple enzymes in higher eukaryotes catalyze H4K20me. PR-Set7/Set8 is responsible for H4K20me1 (Couture et al., 2005; Fang et al., 2002; Nishioka et al., 2002; Xiao et al., 2005), whereas Suv4-20hs are responsible for H4K20me2 and H4K20me3 (Schotta et al., 2004, 2008; Yang et al., 2008). In contrast, in fission yeast *Schizosaccharomyces pombe*, Set9 is the sole enzyme that catalyzes all three states of H4K20me (Sanders et al., 2004), and Set9-mediated H4K20me is required for efficient recruitment of checkpoint

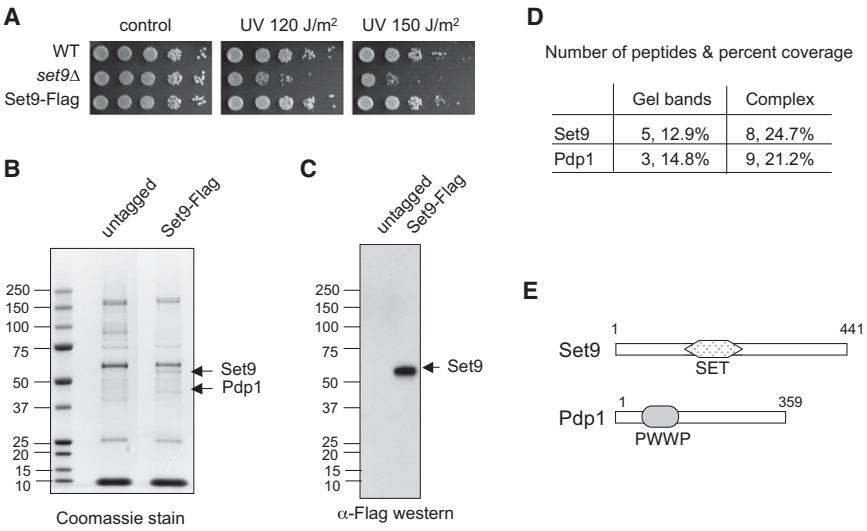

Figure 1. Pdp1 Associates with Set9

(A) Serial dilution plating assays were performed to measure the survival of yeast strains after treatment with indicated doses of UV.

(B) Extracts prepared from wild-type and Set9-Flag strains were used to perform affinity purification with anti-Flag resin, resolved by SDS-PAGE, and stained with Coomassie blue. The identity of protein bands, as determined by mass spectrometry, is indicated on the right.

(C) A portion of the samples, as in (B), was subjected to western blot analysis with Flag antibody.

(D) Mass spectrometry analysis of proteins associated with Flag-Set9. The number of peptides, as well as the percentages of each protein these peptides cover, is indicated.

(E) Schematic diagrams of Set9 and Pdp1. The SET and PWWP domains are indicated.

protein Crb2 to sites of DNA damage (Du et al., 2006; Sanders et al., 2004). This process is highly conserved with the recruitment of 53BP1 (a Crb2 homolog) in mammals (Botuyan et al., 2006). Structural analysis of 53BP1 and Crb2 indicate that they both recognize H4K20me2/H4K20me1, but not H4K20me3, because their binding cavities contain four aromatic residues that prevent the binding of the bulkier trimethylated form (Botuyan et al., 2006). Indeed, biochemical studies demonstrated that 53BP1/Crb2 associates only with H4K20me1 and H4K20me2 (Botuyan et al., 2006; Greeson et al., 2008; Kim et al., 2006), and only H4K20me2 is involved in the recruitment of Crb2 (Greeson et al., 2008). However, the mechanism that regulates Set9 to perform different degrees of H4K20me is poorly understood.

To gain insights into the mechanism underlying the regulation of Set9, we affinity-purified Set9 complex from fission yeast. We found an uncharacterized PWWP (proline-tryptophan-tryptophan-proline) domain-containing protein, Pdp1 (*P*WWP *d*omain *p*rotein *1*), that associates with Set9 and is required for all three states of H4K20me. We demonstrated that Pdp1 interacts with histones and regulates the association of Set9 with chromatin. The PWWP domain belongs to the Royal family (Maurer-Stroh et al., 2003). Members of this family also include Tudor, chromo, and MBT domains, which use aromatic residues to form hydrophobic cavities to interact with methylated histones or chromatin proteins (Maurer-Stroh et al., 2003; Ruthenburg et al., 2007). We discovered that the PWWP domain of Pdp1 binds to H4K20me in vitro and in vivo. Furthermore, mutations of two conserved aromatic residues in a hydrophobic cavity of the PWWP domain abolished this interaction and resulted in the selective loss of H4K20me3 in vivo, establishing that the PWWP domain is a methyl-lysine recognition motif.

RESULTS

Purification of Set9 Complex

To elucidate the mechanism that regulates Set9 function, we generated a yeast strain expressing Set9-Flag driven by its natural promoter from the endogenous chromatin environment. Set9-Flag cells did not show defects in survival after UV treatment and retain H4K20 methylation (Figure 1A and Figure S1 available online), indicating that Set9-Flag is functional. Affinity purification with Flag resin revealed two protein bands that were specifically present in the Set9-Flag purified fraction but were absent in the untagged control fraction (Figure 1B). Mass spectrometry analysis of gel-excised bands identified the protein with a relative molecular mass of 55 KDa as Set9, which was confirmed by western blot analysis (Figure 1C). The protein with a molecular weight of ~40 KDa was identified as SPBC29A3.13, an uncharacterized PWWP domain protein, which we named Pdp1. In addition, mass spectrometry analysis of the Set9-Flag complex by MudPIT analysis (Multidimensional Protein Identification Technology) (Washburn et al., 2001) also identified Pdp1 and Set9 as major components of the complex (Figure 1D).

To confirm the interaction between Pdp1 and Set9 in vivo, we generated strains expressing functional Flag-Pdp1 and Set9-myc at their native chromosomal loci (Figure S1). When protein extracts from cells expressing both Set9-myc and Flag-Pdp1 were used to perform immunoprecipitation analysis, Set9-myc coimmunoprecipitated with Flag-Pdp1 (Figure 2A). In addition, we could immunoprecipitate endogenous Set9 with Flag-Pdp1 (Figure 2B).

Because Pdp1 is the only protein present in stoichiometric amount with Set9 as indicated by Coomassie staining and MudPIT analysis (Figures 1B and 1D), we examined whether these two proteins associate with each other directly using a GST pull-down assay. We found that ^{35}S-labled Pdp1 was retained by GST-Set9 resin, but not control resin with only the GST moiety (Figure 2C). Meanwhile, a control Luciferase (Luc) protein did not interact with GST-Set9 (Figure 2C), demonstrating that the interaction between Set9 and Pdp1 is specific.

Since Pdp1 interacts directly with Set9, we also mapped the domain in Pdp1 that is responsible for this interaction. Interestingly, a fragment of Pdp1 that contains only the PWWP domain (Pdp1-N) failed to interact with GST-Set9 (Figure 2D), although the PWWP domain has been proposed to mediate

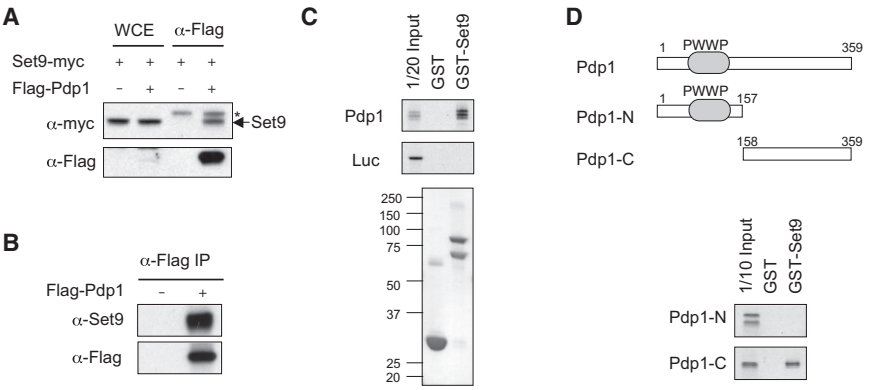

Figure 2. Pdp1 Interacts with Set9 In Vivo and In Vitro

(A and B) Protein extracts prepared from the indicated strains were immunoprecipitated with anti-Flag resin and analyzed by western blot analysis with indicated antibodies. WCE, whole cell extract. Asterisk (*) represents a nonspecific band.

(C) Top: in vitro-translated and ^{35}S-labeled Pdp1 and Luciferase (Luc) were incubated with GST or GST-Set9 immobilized on glutathione beads and washed extensively. The eluted proteins were resolved by SDS-PAGE and imaged by autoradiography. Bottom: purified GST and GST-Set9 were resolved by SDS-PAGE and stained with Coomassie blue.

(D) Top: schematic diagrams of the fragments of Pdp1 used. Bottom: GST pull-down assays were performed as in (C).

protein-protein interactions (Stec et al., 2000). Instead, sequences C-terminal to the PWWP domain of Pdp1 (Pdp1-C) interacted with GST-Set9 (Figure 2D).

Pdp1 Is Essential for H4K20 Methylation

The interaction between Pdp1 and Set9 suggests that Pdp1 might affect Set9-mediated H4K20 methylation. Indeed, western blot analysis of cell extract prepared from *pdp1Δ* strains showed complete loss of mono-, di-, and trimethylation of H4K20, a phenotype identical to that of *set9Δ* strains (Figure 3A). Set9 protein levels were not affected by the loss of Pdp1 (Figure 3B), indicating that Pdp1 regulates the localization or activity of Set9 rather than controlling Set9 stability.

Because the histone methyltransferase activity of Set9 is extremely weak in vitro (data not shown, as noted in an earlier study, Sanders et al. [2004]), we were unable to analyze the effect of Pdp1 on Set9 activity. To examine whether Pdp1 is critical for the recruitment of Set9 to chromatin, we generated a yeast strain expressing H2B-Flag at its endogenous chromosomal locus. Cell extracts from H2B-Flag strains were sonicated to fragment chromatin to an average size of 1 kb and affinity-purified with anti-Flag resin to isolate nucleosomes. We found that Set9 was immunoprecipitated with the nucleosomes, but its association was abolished in the absence of Pdp1 (Figure 3C). We also isolated mononucleosomes by micrococcal nuclease digestion and found that the interaction of Set9 with nucleosomes was also abolished in *pdp1Δ* cells, thus ruling out the possibility that Set9 was associating with higher-order chromatin structures imposed by Pdp1 (Figure S3).

The requirement of Pdp1 for Set9 localization indicates that Pdp1 might directly interact with histones. Consistent with this idea, MudPIT mass spectrometry analysis of affinity purified Flag-Pdp1 identified all of the four core histones (data not shown). Furthermore, when GST-Pdp1 was incubated with HeLa histone octamers, it selectively interacted with histone H3 and H4, which possibly reflect H3/H4 tetramers (Figure 3D).

Pdp1 Is Necessary for DNA-Damage-Checkpoint Activation

In fission yeast, DNA damage activates the sensor kinase Rad3-Rad26 complex (ATR-ATRIP in mammals) (Carr and Casprari, 2003). Rad3 then phosphorylates and activates the effector kinase Chk1, which further triggers a delay in G2-M transition (Carr and Casprari, 2003; Walworth and Bernards, 1996).

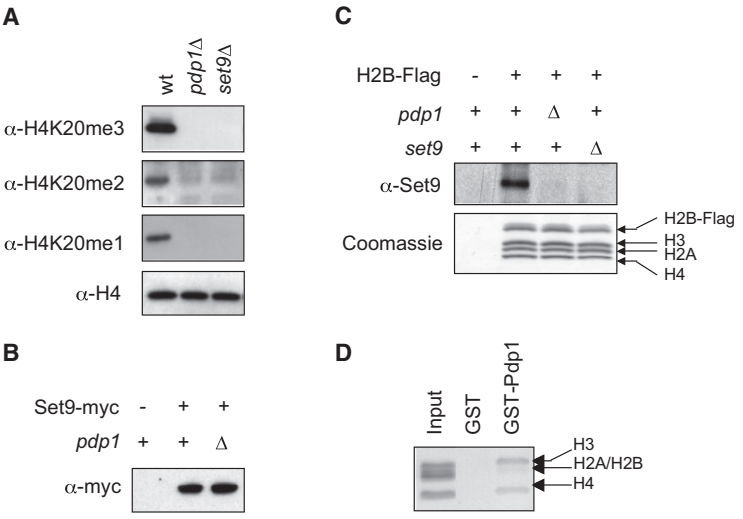

Figure 3. Pdp1 Is Essential for H4K20 Methylation

(A and B) Whole-cell extracts prepared from indicated strains were subjected to western blot analysis with indicated antibodies.

(C) Cell extract from the indicated yeast strains were immunoprecipitated with anti-Flag resin, immunoblotted with Set9 antibody, and stained with Coomassie Blue to visualize histones.

(D) Purified HeLa histone octamers were incubated with GST or GST-Pdp1 immobilized on glutathione beads and washed extensively. The eluted proteins were resolved by SDS-PAGE and stained with Coomassie blue.

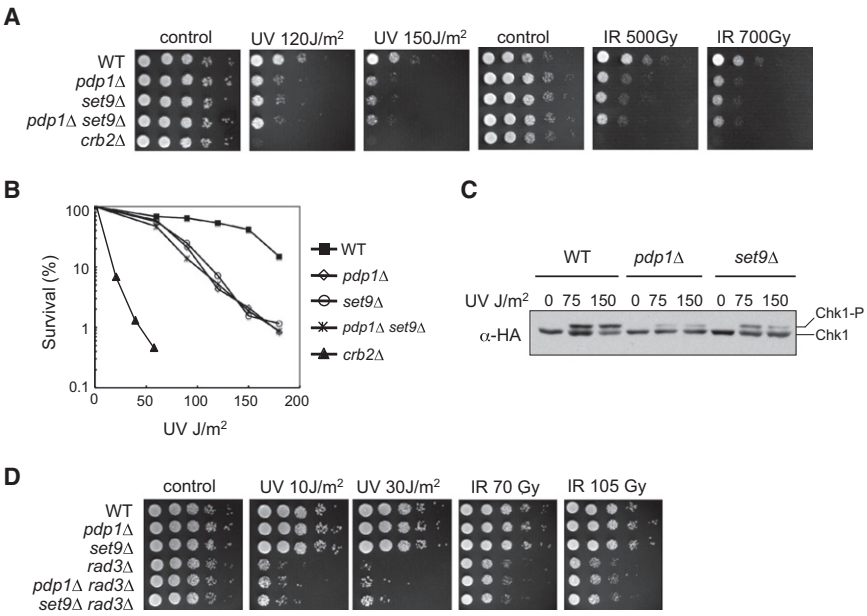

Figure 4. Pdp1 Is Crucial for the Activation of a DNA-Damage Checkpoint

(A) Serial dilution plating assays were performed to measure the survival of yeast strains after treatment with indicated doses of UV and IR.

(B) Survival curves of yeast strains after exposure to UV light.

(C) Yeast strains were treated with indicated doses of UV and immediately processed for western blot analysis with HA antibody to detect Chk1-HA.

(D) Serial dilution plating assays were performed to measure the survival of yeast strains after treatment with indicated doses of UV and IR.

Set9-mediated H4K20 methylation is required for Chk1 phosphorylation to activate the G2-specific DNA-damage checkpoint (Sanders et al., 2004). Yeast cells without Set9 or with a *H4K20R* mutation are sensitive to DNA damage induced by ultraviolet light (UV) or ionizing radiation (IR) (Sanders et al., 2004). Consistent with the idea that Pdp1 and Set9 cooperatively mediate H4K20 methylation, *pdp1Δ* cells showed similar degrees of sensitivity to UV and IR as *set9Δ* cells (Figures 4A and 4B). More importantly, a *set9Δ pdp1Δ* double mutant behaved as either single mutant, indicating that they function in the same pathway genetically (Figures 4A and 4B). Furthermore, both *pdp1Δ H4K20R* and *set9Δ H4K20R* double mutants showed similar degrees of UV sensitivity to that of a *H4K20R* single mutant (Figure S4). Thus, the effects of Pdp1 loss on DNA-damage-checkpoint function are due to the loss of H4K20 methylation. Additionally, DNA-damage-induced phosphorylation of Chk1 is severely compromised in *pdp1Δ* cells (Figure 4C), and a *pdp1Δ rad3Δ* double mutant showed a similar degree of DNA damage sensitivity to that of a *rad3Δ* single mutant (Figure 4D). Collectively, these results demonstrate that Pdp1 is required for the activation of a DNA-damage checkpoint mediated by Rad3-Chk1.

Rad3-mediated phosphorylation of Chk1 requires Crb2, an *S. pombe* homolog of mammalian 53BP1 (Saka et al., 1997) that interacts with H4K20me (Botuyan et al., 2006; Greeson et al., 2008). In response to DNA damage, Crb2 is rapidly recruited to distinct nuclear foci that represent sites of DNA lesions and concomitantly phosphorylated (Du et al., 2003; Saka et al., 1997). Crb2 foci formation and phosphorylation require both methylation of H4K20 and phosphorylation of H2A (H2AX in mammals) at its C-terminal SQ motif (Du et al., 2006; Nakamura et al., 2004; Sanders et al., 2004). Since Pdp1 is essential for H4K20me, we examined whether Pdp1 is directly involved in the recruitment of Crb2 by live cell imaging of cells expressing GFP-Crb2 (Sanders et al., 2004). In wild-type cells, GFP-Crb2 forms distinct foci in addition to a diffuse nuclear staining after treatment of cells with low doses of IR (Figure 5A). However, in the absence of Pdp1, GFP-Crb2 foci are severely reduced (Figure 5A). We also examined the effect of *pdp1Δ* on Crb2 phosphorylation after DNA damage using a strain expressing myc-Crb2 (Sanders et al., 2004). In wild-type cells, Crb2 exhibited a slower migrating form on SDS-PAGE gels after IR treatment (Figure 5B), which represents phosphorylated Crb2 (Saka et al., 1997; Sanders et al., 2004). However, this slow-migrating form of Crb2 is abolished in *pdp1Δ* as well as *set9Δ* cells (Figure 5B), demonstrating that Pdp1 is essential for Crb2 phosphorylation. Since the recruitment and phosphorylation of Crb2 depend on both H4K20me and H2A phosphorylation (Du et al., 2006; Nakamura et al., 2004; Sanders et al., 2004), we also examined the effect of *pdp1Δ* on H2A phosphorylation with a phosphorylated H2A antibody. However, neither *pdp1Δ* nor *set9Δ* affected H2A phosphorylation (Figure 5B), demonstrating that the effect of *Pdp1Δ* on Crb2 localization and phosphorylation is mainly exerted through its effect on H4K20me. Consistent with this idea, both *crb2Δ pdp1Δ* and *crb2Δ set9Δ* double mutants showed similar DNA-damage sensitivity to UV and IR as that of a *crb2Δ* single mutant (Figure 5C).

A Hydrophobic Cavity in the PWWP Domain of Pdp1 Is Crucial for H4K20me3

The PWWP domain is a member of the Royal family, which includes chromo, Tudor, and MBT domains (Maurer-Stroh et al., 2003). Although many of the royal family members bind methylated histones to regulate chromatin dynamics, the function of the PWWP domain is unknown (Maurer-Stroh et al., 2003; Ruthenburg et al., 2007; Stec et al., 2000). Structural studies demonstrated that the chromo, Tudor, and MBT domains use aromatic residues to form hydrophobic cavities to recognize methylated histones (Ruthenburg et al., 2007). Interestingly, the structures of several PWWP domains show that they also form hydrophobic cavities with aromatic residues (Qiu et al., 2002; Slater et al., 2003; Nameki et al., 2005). For example, an *S. pombe* PWWP domain protein of unknown function, SPBC215.07c (Pdp2), contains three highly conserved aromatic residues in the PWWP domain (F136, W139, F169,

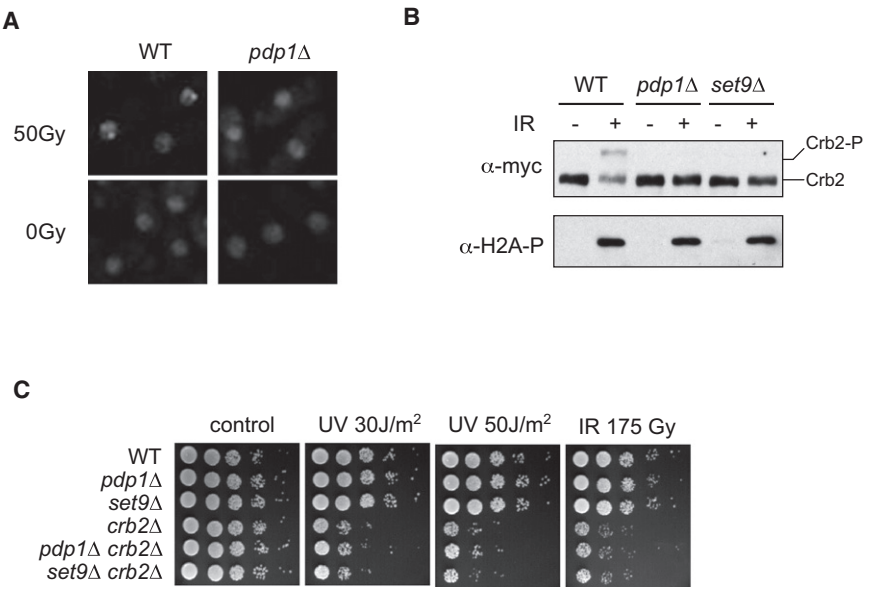

Figure 5. Pdp1 Is Essential for DNA-Damage-Induced Crb2 Foci Formation and Crb2 Phosphorylation

(A) Live cell imaging of yeast strains expressing GFP-Crb2 was performed before and immediately after IR treatment.

(B) The indicated strains were treated with 400 Gy of IR and processed for western blot analysis with myc and phosphorylated H2A antibodies.

(C) Serial dilution plating assays were performed to measure the survival of yeast strains after treatment with indicated doses of UV and IR.

shown in green, blue, and red, respectively, in Figures 6A and 6B), which forms a cavity similar to that of a Tudor domain (Slater et al., 2003). To test whether this hydrophobic cavity is important for the function of Pdp1, we mutated the corresponding residues in Pdp1 into alanines (Y63A, W66A, and F94A). As a control, we also mutated a highly conserved aromatic residue (W65A, corresponding to W138 of Pdp2, shown in pink in Figure 6B), which is close by but faces away from this cavity. We then introduced these mutations together with a 3× Flag tag into the endogenous *Pdp1*$^{+}$ locus. All mutant Pdp1 proteins had similar expression levels as wild-type Pdp1 (Figure 6C), indicating that these mutations do not affect Pdp1 stability. Moreover, immunoprecipitation of Flag-Pdp1 and all of the mutants can efficiently pull down Set9 from cell extracts, demonstrating that these mutants do not affect Pdp1-Set9 association (Figure S5). However, two mutants, W66A and F94A, severely reduced H4K20me3 levels (Figure 6C). As further demonstration of the importance of these aromatic residues, overexpression of W66A and F94A mutants in a wild-type *Pdp1*$^{+}$ background also severely reduced H4K20me3, suggesting that these two mutant forms of Pdp1 could block the function of endogenous Pdp1 (Figure S6). Since Pdp1 is required for the association of Set9 with chromatin, we examined whether these mutants affect Set9 localization as well. Indeed, the association of Set9 with nucleosomes is severely reduced in W66A and F94A mutants (Figure 6D), suggesting that the integrity of the PWWP domain is essential for targeting Set9 to chromatin.

It is surprising that the Y63A mutation behaved differently from W66A and F94A, since it is also located at the same cavity as indicated by the structure of Pdp2 (Slater et al., 2003). However, the structures of other PWWP domains indicate that this residue

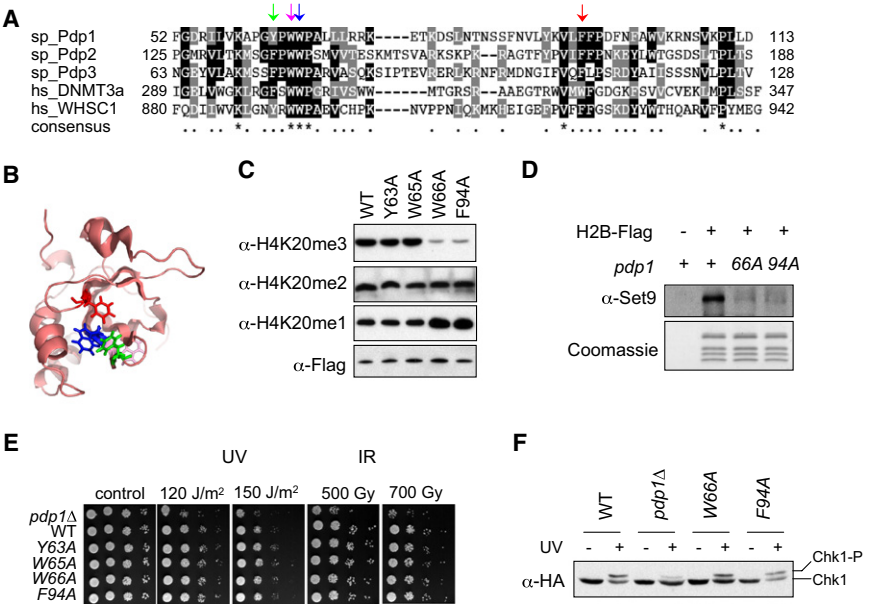

Figure 6. A Hydrophobic Cavity within the PWWP Domain Is Critical for the Function of Pdp1

(A) Sequence alignment of PWWP domain containing proteins. Arrows indicate the positions of amino acids residues mutated in Pdp1.

(B) Ribbon representation of the PWWP domain of fission yeast Pdp2. The side chains of F136, W138, W139, and F169 are shown in green, pink, blue, and red, respectively.

(C) Western blot analysis of cell extracts from indicated strains was performed with H4K20me and Flag antibodies.

(D) Cell extract from the indicated yeast strains were immunoprecipitated with anti-Flag resin, immunoblotted with Set9 antibody, and stained with Coomassie Blue to visualize histones.

(E) Serial dilution plating assays were performed to measure the survival of yeast strains after treatment with indicated doses of UV and IR.

(F) The indicated strains were treated with 150 J/m^2 UV and immediately processed for western blot analysis with HA antibody to detect Chk1-HA.

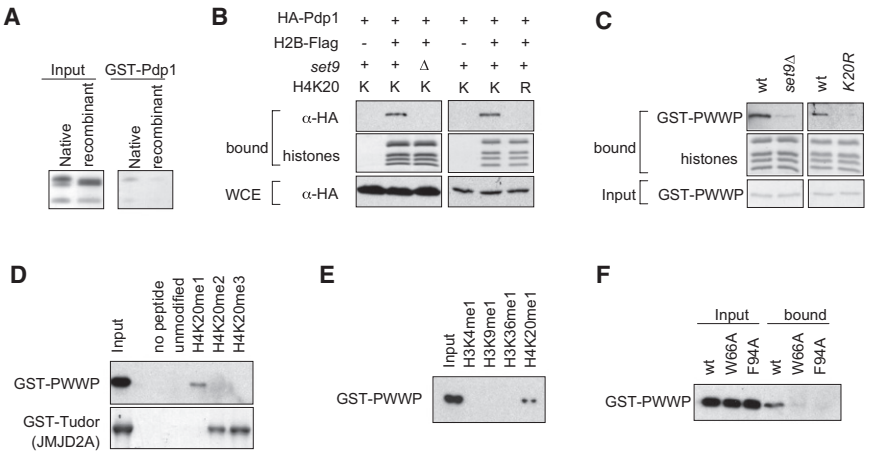

Figure 7. The PWWP Domain of Pdp1 Binds to Methylated H4K20

(A) Purified HeLa histone octamers and recombinant *Xenopus* histone octamers were incubated with GST-Pdp1 immobilized on glutathione beads and washed extensively. The eluted proteins were resolved by SDS-PAGE and stained with Coomassie blue.

(B) Cell extract from the indicated yeast strains was immunoprecipitated with anti-Flag resin to isolate nucleosomes. Bound fractions were immunoblotted with HA antibody and stained with Coomassie blue to visualize histones.

(C) *S. pombe* nucleosomes were purified from indicated strains through H2B-Flag with anti-Flag affinity resin and were incubated with GST-PWWP. Bound fractions were resolved by SDS-PAGE, immunoblotted with a GST antibody, and stained with Coomassie blue to visualize histones.

(D and E) GST-PWWP and GST-Tudor (JMJD2A) were incubated with indicated histone peptides immobilized on agarose resin. Eluted fractions were resolved by SDS-PAGE and immunoblotted with a GST antibody.

(F) GST-PWWP or indicated mutants were incubated with immobilized H4K20me1 peptide, and eluted fractions were immunoblotted with a GST antibody.

shows a high degree of flexibility (Qiu et al., 2002), which might have a different configuration in Pdp1 that is not critical for the integrity of the hydrophobic cavity.

Although H4K20me3 is severely affected in W66A and F94A mutants, H4K20me2 levels were unchanged and there was a significant increase of H4K20me1 (Figure 6C). These results suggest that the PWWP domain of Pdp1 is involved in controlling the activity of Set9 enzyme to regulate the extent of H4K20me. Interestingly, the W66A and F94A mutants were not sensitive to IR or UV (Figure 6E), and Chk1 was efficiently phosphorylated in these cells after UV treatment (Figure 6F), although H4K20me3 was severely compromised. These results indicate that the selective loss of H4K20me3 has no effect on DNA-damage-checkpoint activation, as has been reported recently (Greeson et al., 2008). Since both *set9Δ* and a mutation of H4K20 (*H4K20R*) result in defective checkpoint function, this result indicates that only H4K20me2 or H4K20me1 are involved in DNA-damage-checkpoint control, consistent with biochemical and structural studies demonstrating that 53BP1/Crb2 recognizes H4K20me1 and H4K20me2, but not H4K20me3 (Botuyan et al., 2006; Greeson et al., 2008; Kim et al., 2006).

The PWWP Domain of Pdp1 Binds to H4K20me

As the homologous locations of W66 and F94 on Tudor domain have been implicated in binding to methylated lysines (Maurer-Stroh et al., 2003; Slater et al., 2003), the PWWP domain might recognize methylated histones as well. Supporting this idea, GST-Pdp1 showed reduced binding to histone octamers reconstituted with recombinant histones, which are devoid of any modifications, as compared with native histone octamers purified from HeLa cells (Figure 7A). We reasoned that if Pdp1 interacts with a particular histone methylation through the hydrophobic cavity in the PWWP domain, inactivating the enzyme that catalyzes this modification in vivo would affect H4K20me3, similar to Pdp1 mutants. The fission yeast genome contains 13 putative histone lysine methyltransferases (Set1 through Set13) and 4 putative arginine methyltransferases (Rmt1, Rmt2, Rmt3, and Skb7). Among them, Set1, Set2, Clr4, and Set9 have been shown to methylate histones (Morris et al., 2005; Nakayama et al., 2001; Noma and Grewal, 2002; Sanders et al., 2004). However, except for *set9Δ*, removal of none of the other putative methyltransferases affected H4K20me3 (Figure S7). This result suggests that if Pdp1 interacts with methylated histones, H4K20me might be the only possible target. Supporting this idea, when we examined the association of HA-Pdp1 with chromatin in vivo by pull-down assay with H2B-Flag, we found its chromatin association is abolished by a *set9Δ* or a *H4K20R* mutation (Figure 7B), suggesting that Pdp1 chromatin localization requires H4K20me.

To examine whether the PWWP domain of Pdp1 directly interacts with H4K20me in vitro, we expressed recombinant PWWP domain (1–157) as a GST fusion protein and examined its interaction with yeast nucleosomes isolated through H2B-Flag, which were washed with high stringency to remove nonhistone proteins. We found that the PWWP domain interacted with nucleosomes purified from wild-type cells, but not those from *set9Δ* or *H4K20R* cells, demonstrating that the PWWP domain interacts directly with H4K20me (Figure 7C).

To further probe which degree of H4K20me the PWWP domain interacts with, we performed peptide pull-down assays with H4K20 peptides that contain different degrees of methylation. We found that the PWWP domain only interacts with H4K20me1, but not unmodified H4K20, H4K20me2, or H4K20me3 peptides (Figure 7D). As a control, the Tudor domain of JMJD2A interacts with H4K20me2 and H4K20me3 (Figure 7D) (Kim et al., 2006), demonstrating the integrity of these peptides. In fission yeast, histones are also methylated at H3K4, H3K9, and H3K36; however, the PWWP domain did not interact with peptides monomethylated at these residues (Figure 7E). Furthermore, the W66A and F94A mutants abolished the interaction between the PWWP domain and H4K20me1, demonstrating that the hydrophobic cavity of the PWWP domain is essential for this interaction (Figure 7F).

DISCUSSION

In fission yeast, Set9 is responsible for H4K20 methylation and activation of a DNA-damage checkpoint (Sanders et al., 2004). However, the mechanism that regulates Set9 function is not understood. Using biochemical purification, we identified a PWWP domain-containing protein Pdp1 that associates with Set9 (Figure 1B). Pdp1 is required for all three states of H4K20me in vivo (Figure 3A) and for the activation of a DNA-damage checkpoint (Figure 4 and 5).

We further demonstrated that Pdp1 is required for the association of Set9 with chromatin (Figure 3C). The C-terminal region of Pdp1 mediates association with Set9 (Figure 2D), whereas the N-terminal PWWP domain recognizes H4K20me1 (Figure 7D). Mutations within the PWWP domain that disrupt this interaction (Figure 7E) resulted in the delocalization of Set9 from chromatin (Figure 6D), loss of H4K20me3, and concomitant increase of H4K20me1 (Figure 6C). These results suggest that Pdp1 associates with H4K20me1 to increase the concentration of Set9 on chromatin to perform H4K20me3, whereas the low level of Set9 on chromatin in Pdp1 mutants is sufficient for H4K20me1 and H4K20me2 (Figure 6D). Consistently, overexpression of Set9 in the absence of Pdp1 could rescue H4K20me1 and, to some extent, H4K20me2 (Figure S8), suggesting that Pdp1 is essential for recruiting higher concentration of Set9 to chromatin to perform H4K20me3. Although the weak activity of Set9 in vitro precludes us from determining whether Pdp1 directly regulates Set9 activity (Sanders et al., 2004) (data not shown), our data indicate that the effect of Pdp1 on H4K20me in vivo is mainly exerted through its effect on Set9 chromatin localization.

Interestingly, the loss of H4K20me3 as a result of mutations in the PWWP domain has no effect on DNA-damage-checkpoint function, suggesting that H4K20me2 or H4K20me1, but not H4K20me3, is essential for checkpoint activation (Figures 6E and 6F) (Greeson et al., 2008). This observation is consistent with biochemical and structural studies that demonstrate the preferential association of 53BP1/Crb2 with H4K20me2, but not H4K20me3 (Botuyan et al., 2006; Greeson et al., 2008; Kim et al., 2006). In higher eukaryotes, H4K20me3 is mainly enriched at heterochromatin and is required for proper heterochromatin assembly (Schotta et al., 2004). However, in fission yeast, H4K20me3 is broadly distributed across the genome (Sanders et al., 2004). The function of H4K20me3 in fission yeast is currently unknown, as no phenotypes of *pdp1*$^{+}$ mutant cells were observed under various stress conditions (data not shown). This is consistent with a previous report that *set9Δ* has no effect on gene expression or stress response other than DNA-damage-checkpoint function (Sanders et al., 2004). However, our ability to manipulate methylation states with Pdp1 mutations offers a unique opportunity to further probe the role of H4K20me3 on cellular functions.

In mammals, several HMTases, such as NSD1 and NSD2, contain PWWP domains (Stec et al., 2000). NSD1 is known to methylate H4K20 and H3K36 and is required for early embryonic development (Rayasam et al., 2003). Whether the PWWP domain contributes to the regulation of these enzymes is currently unknown, but it seems a general theme that chromatin-binding domains regulate associated HMTase activities. For example, the mammalian H4K20 methyltransferase Suv4-20 associates with chromo domain protein HP1, which binds to H3K9me and is required for H4K20me3 (Schotta et al., 2004). Similarly, the H3K9 methyltransferase Clr4 contains a chromo domain that recognizes H3K9me to promote the spread of this modification across large chromosomal domains (Zhang et al., 2008).

The PWWP domain is present in diverse proteins involved in chromatin function, including histone-modifying enzymes, DNA-modifying enzymes, transcription factors, and DNA-repair proteins (Stec et al., 2000). Apart from Pdp1, fission yeast contains two other PWWP domain proteins, Pdp2 and Pdp3 (SPAC23D3.01), of unknown function. Although they share strong homology with Pdp1 even outside the PWWP domain, the removal of Pdp2 or Pdp3 had no effect on H4K20 methylation or sensitivity to DNA-damage treatments, suggesting that they participate in distinct cellular processes (Figure S9). The PWWP domain was previously shown to bind histones or DNA (Qiu et al., 2002; Laue et al., 2008); however, its function is still unclear. The homology between PWWP, Tudor, chromo, and MBT domains suggests that the PWWP domain might recognize methylated histones as well (Maurer-Stroh et al., 2003; Ruthenburg et al., 2007). However, previous analysis with a protein array containing PWWP domains failed to detect any interaction with methylated histone peptides (Kim et al., 2006). It should be noted that only a limited number of PWWP domains and methylated histone peptides were tested for binding (Kim et al., 2006). In addition, a recent comparison of the protein array method with peptide pull-down assays or isothermal titration calorimetry demonstrates that the array method is less sensitive (Shi et al., 2007). Our analysis demonstrated that the PWWP domain of Pdp1 binds to H4K20me in vivo and in vitro (Figure 7), suggesting that methyl-lysine recognition might be a general characteristic of PWWP domains.

It is interesting to note that the PWWP domain is only present in eukaryotes and is often associated with chromatin function (Stec et al., 2000). This suggests that the PWWP domain might have coevolved with chromatin as a regulator of chromatin organization. Our analyses demonstrate that, consistent with structural predictions (Maurer-Stroh et al., 2003), the PWWP domain is a new member of the ever-expanding family of motifs that recognize methylated lysines. Interestingly, variations exist in PWWP domains. For example, the NSD1 family of histone methyltransferases often contains a RWWP motif, whereas DNMT3a/b contains an SWWP motif, which results in significant structural variations (Slater et al., 2003) (Figure 6A). The large number of PWWP domain proteins and these structural variations make them ideal for recognizing different residues and/or degrees of histone methylation. Further analysis to elucidate the binding specificity of this domain in other proteins will greatly improve our understanding of the complicated network of histone covalent modifications.

EXPERIMENTAL PROCEDURES

Fission Yeast Strains

Set9-Flag, Set9-myc, *set9Δ*, *pdp1Δ*, and Htb1-Flag strains were constructed using a PCR-based module method (Bahler et al., 1998). Flag-Pdp1 and

HA-Pdp1 strains were generated by first inserting a *ura4*$^+$ gene in the promoter region of *Pdp1*$^+$ and subsequently replacing it with 3× Flag or 3× HA sequences. The Y63A, W65A, W66A, and F94A mutations of *Pdp1*$^+$ were generated with the QuickChange site-directed mutagenesis kit (Stratagene) and were introduced similarly into the *pdp1*$^+$ locus.

Protein Purification and Immunoprecipitation

For affinity purification of Set9-Flag associated proteins, 12 l of wild-type and Set9-Flag cells were harvested, washed with 2× HC buffer (300 mM HEPES-KOH [pH 7.6], 2 mM EDTA, 100 mM KCl, 20% glycerol, 2 mM DTT, and protease inhibitor cocktail [Roche]) and frozen in liquid nitrogen. Crude cell extracts were prepared by vigorously blending frozen yeast cells with dry ice using a household blender, followed by incubation with 40 ml 1× HC buffer containing 250 mM KCl for 30 min. The lysate was cleared by centrifugation at 82,700 g for 2 hr. The supernatants were precleared with proteinA-agarose, then incubated with 200 μl of Flag-agarose for 4 hr and washed eight times with 1× HC containing 250 mM KCl. Bound proteins were eluted with 200 mg/ml 3× Flag peptide, precipitated by TCA, resolved by SDS–PAGE and stained with Coomassie blue.

Mass Spectrometry Analysis

Sample preparation and MudPIT analysis of protein complexes were performed using an LCQ-Deca mass spectrometer (ThremoFinnigan) as previously described (Washburn et al., 2001). MS/MS spectra were submitted to SGD *Schizosaccharomyces pombe* (ver. 10-12-06) protein sequence database searching with the SEQUEST algorithm (Eng et al., 1994).

Protein-Protein Interaction Assays

Purification of GST-Set9 and GST-PWWP fusion proteins was performed according to the manufacturer's protocols (GE). Pdp1 was labeled with [^{35}S]methionine with the TNT T7 coupled reticulocyte lysate system (Promega). For the binding assays, 2 μg of a GST-Set9 fusion protein was immobilized on glutathione-agarose beads in 400 μl HEMNK buffer (40 mM HEPES [pH 7.6], 0.2 mM EDTA, 5 mM $MgCl_2$, 0.5% NP40, 100 mM KCl, and 1 mM DTT) and incubated with 10 μl of in vitro translation products for 1 hr at 4°C. The beads were washed five times with 1 ml of HEMNK, eluted with sample buffer, and resolved by SDS-PAGE. The gel was then dried and exposed to film.

Western Blots and Antibodies

Protein extracts were prepared by lysing cells with glass beads, followed by sonication to dissolve chromatin. The following antibodies were used for western blot analyses: H4K20me1 (Abcam, ab9051), H4K20me2 (Abcam, ab9052 and Upstate, 07-367), H4K20me3 (Abcam, ab9053), Set9 (Abcam, ab3826), phospho-H2A (Abcam, ab15083), myc (Covance, MMP-150), HA (Roche, 12013819001), GST (Sigma, G7781), and Flag (Sigma, F7425).

DNA-Damage-Sensitivity Assays

For IR and UV treatment, serial dilutions of cells were plated onto YEA plates and irradiated with a ^{137}Cs source at a dose of 7 Gy/min or a UVP CL-1000 crosslinker (254 nm) and incubated for 3 days at 30°C. For survival rate analysis, cells were plated at a density of 500–2000 cells/plate and irradiated with UV. Colonies were counted after 3 days at 30°C and normalized to colony numbers without UV treatment. All strains used to test DNA-damage sensitivity are *ura4*$^+$. Analysis of Chk1, Crb2, and H2A phosphorylation after UV treatment was performed as described previously (Walworth and Bernards, 1996).

In Vivo Chromatin-Binding Assays

In vivo chromatin-binding assays of Set9 or HA-Pdp1 were performed with yeast cells expressing H2B-Flag. Mid-log-phase cultures of yeast cells were transferred to 18°C and treated with 3% paraformaldehyde for 30 min. The fixed cells were then lysed with acid-washed glass beads in ChIP lysis buffer (50 mM HEPES [pH 7.5], 140 mM NaCl, 1% TritonX-10, 0.1% deoxycholate sodium, 1 mM PMSF, and protease inhibitor cocktail [Roche]). Sonicated chromatin were incubated with Flag-agarose resin, washed extensively, and boiled in SDS loading buffer to reverse crosslinking. The eluted fractions were subjected to western blot analysis with Set9 or HA antibodies and Coomassie staining to visualize histones.

In Vitro Nucleosome-Binding Assays

To obtain *S. pombe* nucleosomes, extracts of yeast cells expressing H2B-Flag were sonicated to fragment chromatin, incubated with Flag-agarose in 1× HC buffer (150 mM HEPES-KOH [pH 7.6], 1 mM EDTA, 10% glycerol, 0.5% NP-40, 1 mM DTT, protease inhibitor cocktail [Roche]) containing 400 mM KCl, and extensively washed. PWWP or mutants were expressed as GST fusion proteins, purified according to manufacturer's protocols (GE), and further purified by gel filtration with a Superdex S-200 column. Nucleosomes immobilized on Flag-agarose beads were then incubated with 1 μg of purified proteins in 1× HC buffer containing 200 mM KCl at 4°C for 4 hr, washed five times with 1× HC (200 mM KCl). Bound fractions were resolved by SDS-PAGE, and western blot analysis was performed with a GST antibody.

Peptide Pull-Down Assays

Histone peptides containing different degrees of H4K20 methylation (Abcam ab14963, ab17043, ab14964, and ab17567), H3K4me1 (ab1340), H3K9me1 (ab1771), or H3K36me1 (ab1783) were immobilized on agarose resin with SulforLink Immobilization Kit for peptides according to the manufacturer's protocol (Thermo, 44999). For peptide pull-down assays, 1 μg of GST-PWWP, GST-PWWP-W66A, or GST-PWWP-F94A proteins were incubated with 1 μg of immobilized peptides in 1× HC buffer containing 200 mM KCl for 4 hr at 4°C and washed extensively. Bound proteins were eluted with 100 mM glycine (pH 2.8), resolved by SDS-PAGE, and western blot analyses were performed with a GST antibody.

SUPPLEMENTAL DATA

The Supplemental Data include nine figures and can be found with this article online at http://www.cell.com/molecular-cell/supplemental/S1097-2765(09)00078-1.

ACKNOWLEDGMENTS

We thank S. Kallgren, M. Natalia, and V. Ringgold for assistance with strain construction. We thank S. Grewal for providing strains and plasmids. *set9Δ*, *Set9-Myc*, and *Set9-Flag* strains used in this study were constructed in the Grewal laboratory. We thank N. Walworth, S. Sanders, S. Marcus, P. Silver, F. Chang, and M. Bedford for strains and plasmids; A. Verreault and M. Yanagida for antibodies; A. Courey and B. Strahl for nucleosomes; Y. Shi for histone peptides; L. Tong and C. Wang for help with structural analysis; R. Rothstein, J. Barlow, and J. Sable for help with microscopy; L. Tong and Y. Bai for help with gel filtration analysis; and J. Hunt and B. Ergel for help with peptide interaction assays. We thank J. Manley, C. Prives, L. Chasin, S. Grewal, and S. Kallgren for critical reading of the manuscript. This work is supported by a Basal O'Connor Starter Scholar Award from the March of Dimes foundation and NIH grant R01 GM085145 to S.J. and by the National Center for Research Resources of the National Institutes of Health by a grant to T.N.D (P41 RR11823).

Received: October 29, 2007
Revised: May 18, 2008
Accepted: February 4, 2009
Published: February 26, 2009

REFERENCES

Bahler, J., Wu, J.Q., Longtine, M.S., Shah, N.G., McKenzie, A., 3rd, Steever, A.B., Wach, A., Philippsen, P., and Pringle, J.R. (1998). Heterologous modules for efficient and versatile PCR-based gene targeting in Schizosaccharomyces pombe. Yeast *14*, 943–951.

Berger, S.L. (2007). The complex language of chromatin regulation during transcription. Nature *447*, 407–412.

Botuyan, M.V., Lee, J., Ward, I.M., Kim, J.E., Thompson, J.R., Chen, J., and Mer, G. (2006). Structural basis for the methylation state-specific recognition of histone H4–K20 by 53BP1 and Crb2 in DNA repair. Cell *127*, 1361–1373.

Cao, R., Wang, L., Wang, H., Xia, L., Erdjument-Bromage, H., Tempst, P., Jones, R.S., and Zhang, Y. (2002). Role of histone H3 lysine 27 methylation in Polycomb-group silencing. Science *298*, 1039–1043.

Carr, A.M., and Casprari, T. (2003). Checkpoint conrols halting the cell cycle. In The Molecular Biology of Schizosaccharomyces pombe, R. Egel, ed. (Berlin: Springer), pp. 41–56.

Couture, J.F., Collazo, E., Brunzelle, J.S., and Trievel, R.C. (2005). Structural and functional analysis of SET8, a histone H4 Lys-20 methyltransferase. Genes Dev. *19*, 1455–1465.

Czermin, B., Melfi, R., McCabe, D., Seitz, V., Imhof, A., and Pirrotta, V. (2002). *Drosophila* enhancer of Zeste/ESC complexes have a histone H3 methyltransferase activity that marks chromosomal Polycomb sites. Cell *111*, 185–196.

Downs, J.A., Nussenzweig, M.C., and Nussenzweig, A. (2007). Chromatin dynamics and the preservation of genetic information. Nature *447*, 951–958.

Du, L.L., Nakamura, T.M., Moser, B.A., and Russell, P. (2003). Retention but not recruitment of Crb2 at double-strand breaks requires Rad1 and Rad3 complexes. Mol. Cell. Biol. *23*, 6150–6158.

Du, L.L., Nakamura, T.M., and Russell, P. (2006). Histone modification-dependent and -independent pathways for recruitment of checkpoint protein Crb2 to double-strand breaks. Genes Dev. *20*, 1583–1596.

Eng, J., McCormack, A., and Yates, J.R., 3rd. (1994). An approach to correlate tandem mass spectral data of peptides with amino acid sequences in a protein database. J. Am. Soc. Mass Spectrom. *5*, 976–989.

Fang, J., Feng, Q., Ketel, C.S., Wang, H., Cao, R., Xia, L., Erdjument-Bromage, H., Tempst, P., Simon, J.A., and Zhang, Y. (2002). Purification and functional characterization of SET8, a nucleosomal histone H4-lysine 20-specific methyltransferase. Curr. Biol. *12*, 1086–1099.

Greeson, N.T., Sengupta, R., Arida, A.R., Jenuwein, T., and Sanders, S.L. (2008). Di-methyl H4 lysine 20 targets the checkpoint protein CRB2 to sites of DNA damage. J. Biol. Chem. *283*, 33168–33174.

Groth, A., Rocha, W., Verreault, A., and Almouzni, G. (2007). Chromatin challenges during DNA replication and repair. Cell *128*, 721–733.

Hong, E.J., Villen, J., Gerace, E.L., Gygi, S.P., and Moazed, D. (2005). A Cullin E3 Ubiquitin Ligase Complex Associates with Rik1 and the Clr4 Histone H3–K9 Methyltransferase and Is Required for RNAi-Mediated Heterochromatin Formation. RNA Biol. *2*, 106–111.

Horn, P.J., Bastie, J.N., and Peterson, C.L. (2005). A Rik1-associated, cullin-dependent E3 ubiquitin ligase is essential for heterochromatin formation. Genes Dev. *19*, 1705–1714.

Huyen, Y., Zgheib, O., Ditullio, R.A., Jr., Gorgoulis, V.G., Zacharatos, P., Petty, T.J., Sheston, E.A., Mellert, H.S., Stavridi, E.S., and Halazonetis, T.D. (2004). Methylated lysine 79 of histone H3 targets 53BP1 to DNA double-strand breaks. Nature *432*, 406–411.

Jia, S., Kobayashi, R., and Grewal, S.I. (2005). Ubiquitin ligase component Cul4 associates with Clr4 histone methyltransferase to assemble heterochromatin. Nat. Cell Biol. *7*, 1007–1013.

Julien, E., and Herr, W. (2004). A switch in mitotic histone H4 lysine 20 methylation status is linked to M phase defects upon loss of HCF-1. Mol. Cell *14*, 713–725.

Karachentsev, D., Sarma, K., Reinberg, D., and Steward, R. (2005). PR-Set7-dependent methylation of histone H4 Lys 20 functions in repression of gene expression and is essential for mitosis. Genes Dev. *19*, 431–435.

Kim, J., Daniel, J., Espejo, A., Lake, A., Krishna, M., Xia, L., Zhang, Y., and Bedford, M.T. (2006). Tudor, MBT and chromo domains gauge the degree of lysine methylation. EMBO Rep. *7*, 397–403.

Kouzarides, T. (2007). Chromatin modifications and their function. Cell *128*, 693–705.

Kuzmichev, A., Nishioka, K., Erdjument-Bromage, H., Tempst, P., and Reinberg, D. (2002). Histone methyltransferase activity associated with a human multiprotein complex containing the Enhancer of Zeste protein. Genes Dev. *16*, 2893–2905.

Laue, K., Daujat, S., Crump, J.G., Plaster, N., Roehl, H.H., Kimmel, C.B., Schneider, R., and Hammerschmidt, M. (2008). The multidomain protein Brpf1 binds histones and is required for Hox gene expression and segmental identity. Development *135*, 1935–1946.

Li, B., Carey, M., and Workman, J.L. (2007). The role of chromatin during transcription. Cell *128*, 707–719.

Litt, M.D., Simpson, M., Gaszner, M., Allis, C.D., and Felsenfeld, G. (2001). Correlation between histone lysine methylation and developmental changes at the chicken beta-globin locus. Science *293*, 2453–2455.

Luger, K., Mader, A.W., Richmond, R.K., Sargent, D.F., and Richmond, T.J. (1997). Crystal structure of the nucleosome core particle at 2.8 A resolution. Nature *389*, 251–260.

Martin, C., and Zhang, Y. (2005). The diverse functions of histone lysine methylation. Nat. Rev. Mol. Cell Biol. *6*, 838–849.

Maurer-Stroh, S., Dickens, N.J., Hughes-Davies, L., Kouzarides, T., Eisenhaber, F., and Ponting, C.P. (2003). The Tudor domain 'Royal Family': Tudor, plant Agenet, Chromo, PWWP and MBT domains. Trends Biochem. Sci. *28*, 69–74.

Morris, S.A., Shibata, Y., Noma, K., Tsukamoto, Y., Warren, E., Temple, B., Grewal, S.I., and Strahl, B.D. (2005). Histone H3 K36 methylation is associated with transcription elongation in Schizosaccharomyces pombe. Eukaryot. Cell *4*, 1446–1454.

Muller, J., Hart, C.M., Francis, N.J., Vargas, M.L., Sengupta, A., Wild, B., Miller, E.L., O'Connor, M.B., Kingston, R.E., and Simon, J.A. (2002). Histone methyltransferase activity of a *Drosophila* Polycomb group repressor complex. Cell *111*, 197–208.

Nakamura, T.M., Du, L.L., Redon, C., and Russell, P. (2004). Histone H2A phosphorylation controls Crb2 recruitment at DNA breaks, maintains checkpoint arrest, and influences DNA repair in fission yeast. Mol. Cell. Biol. *24*, 6215–6230.

Nakayama, J., Rice, J.C., Strahl, B.D., Allis, C.D., and Grewal, S.I. (2001). Role of histone H3 lysine 9 methylation in epigenetic control of heterochromatin assembly. Science *292*, 110–113.

Nameki, N., Tochio, N., Koshiba, S., Inoue, M., Yabuki, T., Aoki, M., Seki, E., Matsuda, T., Fujikura, Y., Saito, M., et al. (2005). Solution structure of the PWWP domain of the hepatoma-derived growth factor family. Protein Sci. *14*, 756–764.

Nishioka, K., Rice, J.C., Sarma, K., Erdjument-Bromage, H., Werner, J., Wang, Y., Chuikov, S., Valenzuela, P., Tempst, P., Steward, R., et al. (2002). PR-Set7 is a nucleosome-specific methyltransferase that modifies lysine 20 of histone H4 and is associated with silent chromatin. Mol. Cell *9*, 1201–1213.

Noma, K., Allis, C.D., and Grewal, S.I. (2001). Transitions in distinct histone H3 methylation patterns at the heterochromatin domain boundaries. Science *293*, 1150–1155.

Noma, K., and Grewal, S.I. (2002). Histone H3 lysine 4 methylation is mediated by Set1 and promotes maintenance of active chromatin states in fission yeast. Proc. Natl. Acad. Sci. USA *99* (*Suppl 4*), 16438–16445.

Qiu, C., Sawada, K., Zhang, X., and Cheng, X. (2002). The PWWP domain of mammalian DNA methyltransferase Dnmt3b defines a new family of DNA-binding folds. Nat. Struct. Biol. *9*, 217–224.

Rayasam, G.V., Wendling, O., Angrand, P.O., Mark, M., Niederreither, K., Song, L., Lerouge, T., Hager, G.L., Chambon, P., and Losson, R. (2003). NSD1 is essential for early post-implantation development and has a catalytically active SET domain. EMBO J. *22*, 3153–3163.

Rice, J.C., Nishioka, K., Sarma, K., Steward, R., Reinberg, D., and Allis, C.D. (2002). Mitotic-specific methylation of histone H4 Lys 20 follows increased PR-Set7 expression and its localization to mitotic chromosomes. Genes Dev. *16*, 2225–2230.

Rouse, J., and Jackson, S.P. (2002). Interfaces between the detection, signaling, and repair of DNA damage. Science *297*, 547–551.

Ruthenburg, A.J., Allis, C.D., and Wysocka, J. (2007). Methylation of lysine 4 on histone H3: intricacy of writing and reading a single epigenetic mark. Mol. Cell *25*, 15–30.

Saka, Y., Esashi, F., Matsusaka, T., Mochida, S., and Yanagida, M. (1997). Damage and replication checkpoint control in fission yeast is ensured by interactions of Crb2, a protein with BRCT motif, with Cut5 and Chk1. Genes Dev. *11*, 3387–3400.

Sakaguchi, A., and Steward, R. (2007). Aberrant monomethylation of histone H4 lysine 20 activates the DNA damage checkpoint in *Drosophila melanogaster*. J. Cell Biol. *176*, 155–162.

Sanders, S.L., Portoso, M., Mata, J., Bahler, J., Allshire, R.C., and Kouzarides, T. (2004). Methylation of histone H4 lysine 20 controls recruitment of Crb2 to sites of DNA damage. Cell *119*, 603–614.

Schotta, G., Lachner, M., Sarma, K., Ebert, A., Sengupta, R., Reuter, G., Reinberg, D., and Jenuwein, T. (2004). A silencing pathway to induce H3–K9 and H4–K20 trimethylation at constitutive heterochromatin. Genes Dev. *18*, 1251–1262.

Schotta, G., Sengupta, R., Kubicek, S., Malin, S., Kauer, M., Callen, E., Celeste, A., Pagani, M., Opravil, S., De La Rosa-Velazquez, I.A., et al. (2008). A chromatin-wide transition to H4K20 monomethylation impairs genome integrity and programmed DNA rearrangements in the mouse. Genes Dev. *22*, 2048–2061.

Shi, X., Kachirskaia, I., Walter, K.L., Kuo, J.H., Lake, A., Davrazou, F., Chan, S.M., Martin, D.G., Fingerman, I.M., Briggs, S.D., et al. (2007). Proteome-wide analysis in Saccharomyces cerevisiae identifies several PHD fingers as novel direct and selective binding modules of histone H3 methylated at either lysine 4 or lysine 36. J. Biol. Chem. *282*, 2450–2455.

Slater, L.M., Allen, M.D., and Bycroft, M. (2003). Structural variation in PWWP domains. J. Mol. Biol. *330*, 571–576.

Stec, I., Nagl, S.B., van Ommen, G.J., and den Dunnen, J.T. (2000). The PWWP domain: a potential protein-protein interaction domain in nuclear proteins influencing differentiation? FEBS Lett. *473*, 1–5.

Walworth, N.C., and Bernards, R. (1996). rad-dependent response of the chk1-encoded protein kinase at the DNA damage checkpoint. Science *271*, 353–356.

Wang, H., An, W., Cao, R., Xia, L., Erdjument-Bromage, H., Chatton, B., Tempst, P., Roeder, R.G., and Zhang, Y. (2003). mAM facilitates conversion by ESET of dimethyl to trimethyl lysine 9 of histone H3 to cause transcriptional repression. Mol. Cell *12*, 475–487.

Washburn, M.P., Wolters, D., and Yates, J.R., III. (2001). Large-scale analysis of the yeast proteome by multidimensional protein identification technology. Nat. Biotechnol. *19*, 242–247.

Wysocka, J., Swigut, T., Milne, T.A., Dou, Y., Zhang, X., Burlingame, A.L., Roeder, R.G., Brivanlou, A.H., and Allis, C.D. (2005). WDR5 associates with histone H3 methylated at K4 and is essential for H3 K4 methylation and vertebrate development. Cell *121*, 859–872.

Xiao, B., Jing, C., Kelly, G., Walker, P.A., Muskett, F.W., Frenkiel, T.A., Martin, S.R., Sarma, K., Reinberg, D., Gamblin, S.J., and Wilson, J.R. (2005). Specificity and mechanism of the histone methyltransferase Pr-Set7. Genes Dev. *19*, 1444–1454.

Yang, H., Pesavento, J.J., Starnes, T.W., Cryderman, D.E., Wallrath, L.L., Kelleher, N.L., and Mizzen, C.A. (2008). Preferential dimethylation of histone H4 lysine 20 by Suv4–20. J. Biol. Chem. *283*, 12085–12092.

Zhang, K., Mosch, K., Fischle, W., and Grewal, S.I. (2008). Roles of the Clr4 methyltransferase complex in nucleation, spreading and maintenance of heterochromatin. Nat. Struct. Mol. Biol. *15*, 381–388.

Zhou, B.B., and Elledge, S.J. (2000). The DNA damage response: putting checkpoints in perspective. Nature *408*, 433–439.